



Article

HWA1- and HWA2-Mediated Hybrid Weakness in Rice Involves Cell Death, Reactive Oxygen Species Accumulation, and Disease Resistance-Related Gene Upregulation

Kumpei Shiragaki ¹, Takahiro Iizuka ¹, Katsuyuki Ichitani ², Tsutomu Kuboyama ³ , Toshinobu Morikawa ¹, Masayuki Oda ¹ and Takahiro Tezuka ^{1,4,*} 

¹ Graduate School of Life and Environmental Sciences, Osaka Prefecture University, 1-1 Gakuen-cho, Nakaku, Sakai, Osaka 599-8531, Japan; ma201027@edu.osakafu-u.ac.jp (K.S.); ddlfte@gmail.com (T.I.); d-morikawa@hannan-u.ac.jp (T.M.); masa-oda@d.email.ne.jp (M.O.)

² Faculty of Agriculture, Kagoshima University, 1-21-24 Korimoto, Kagoshima, Kagoshima 890-0065, Japan; ichitani@agri.kagoshima-u.ac.jp

³ College of Agriculture, Ibaraki University, 3-21-1 Chuo, Ami, Ibaraki 300-0393, Japan; tsutomu.kuboyama.a@vc.ibaraki.ac.jp

⁴ Education and Research Field, College of Life, Environment, and Advanced Sciences, Osaka Prefecture University, 1-1 Gakuen-cho, Nakaku, Sakai, Osaka 599-8531, Japan

* Correspondence: tezuka@plant.osakafu-u.ac.jp; Tel.: +81-72-254-8457

Received: 28 August 2019; Accepted: 24 October 2019; Published: 25 October 2019



Abstract: Hybrid weakness is a type of reproductive isolation in which F₁ hybrids of normal parents exhibit weaker growth characteristics than their parents. F₁ hybrid of the *Oryza sativa* Indian cultivars ‘P.T.B.7’ and ‘A.D.T.14’ exhibits hybrid weakness that is associated with the *HWA1* and *HWA2* loci. Accordingly, the aim of the present study was to analyze the hybrid weakness phenotype of the ‘P.T.B.7’ × ‘A.D.T.14’ hybrids. The height and tiller number of the F₁ hybrid were lower than those of either parent, and F₁ hybrid also exhibited leaf yellowing that was not observed in either parent. In addition, the present study demonstrates that SPAD values, an index correlated with chlorophyll content, are effective for evaluating the progression of hybrid weakness that is associated with the *HWA1* and *HWA2* loci because it accurately reflects degree of leaf yellowing. Both cell death and H₂O₂, a reactive oxygen species, were detected in the yellowing leaves of the F₁ hybrid. Furthermore, disease resistance-related genes were upregulated in the yellowing leaves of the F₁ hybrids, whereas photosynthesis-related genes tended to be downregulated. These results suggest that the hybrid weakness associated with the *HWA1* and *HWA2* loci involves hypersensitive response-like mechanisms.

Keywords: *Oryza sativa*; hybrid weakness; cell death; reactive oxygen species; leaf yellowing; SPAD; hypersensitive response

1. Introduction

The traits of existing crop cultivars can be improved by crossing cultivars or lines to introduce beneficial traits, such as resistance or tolerance to disease or stress, to susceptible cultivars. However, because reproductive isolation mechanisms can hinder the production of hybrids, methods must be developed to overcome the underlying mechanisms of such reproductive isolation.

One type of post-zygotic reproductive isolation, namely hybrid weakness (i.e., hybrid lethality or hybrid necrosis). F₁ hybrids that exhibit this phenomenon are characterized by weaker growth than

their parents, and the phenomenon has been reported to occur in the offspring of crosses involved a number of species, including *Oryza sativa* [1–4], *Nicotiana* spp. [5], *Capsicum* spp. [6], *Arabidopsis thaliana* [7], *Triticum* spp. [8,9], *Gossypium* spp. [10], and *Phaseolus vulgaris* [11]. The genetic mechanisms of hybrid weakness are explained by the Bateson–Dobzhansky–Muller model [12–14], which posits that the reduced hybrid vigor is driven by deleterious interactions between genes at different loci. In many cases, one of the causal genes is related to disease resistance (*R*), and interactions between the *R* gene and other causal gene cause autoimmune responses in the hybrid offspring [2,7]. The autoimmune responses include the accumulation of reactive oxygen species such as H₂O₂, cell death, upregulation of disease resistance-related genes, and downregulation of photosynthesis-related genes [2,7,15,16].

In rice, hybrid weakness has been reported to result from interactions between the *HWI1* locus, which encodes the LRR-RLK gene (*R* gene), and the *HWI2* locus, which encodes a subtilisin-like protease, and hybrids have been reported to exhibit localized programmed cell death (PCD), the high accumulation of salicylic and jasmonic acids, and amplified heat-related weakness symptoms [2]. These results demonstrate that the interaction of causal genes can activate downstream immune responses, such as hypersensitive response-like mechanisms [2,7].

The hybrid weakness that results from the interaction of *Hwa1-1*, a dominant allele of the *HWA1* locus, and *Hwa2-1*, a dominant allele of the *HWA2* locus, was firstly reported in rice by Oka [4]. In that study, F₁ hybrid seedlings that exhibited hybrid weakness were reported to exhibit normal germination and seedling growth until developing three to four leaves, after which plant growth halted and the leaves yellowed. Then, unless the environment was particularly favorable, the plants died before reaching anthesis. The distributions of the *Hwa1-1* and *Hwa2-1* alleles were limited to Indian cultivars [4], and both the *HWA1* and *HWA2* loci were located in a 1637-kb region of the long arm of chromosome 11 [17]. However, the causal genes have not been identified, and the molecular mechanism underlying the hybrid weakness associated with the *HWA1* and *HWA2* loci remain unclear.

Accordingly, the aim of the present study was to characterize the phenotypes of the hybrid weakness that is associated with the *HWA1* and *HWA2* loci, in order to understand the system's underlying mechanisms. The effectiveness of SPAD values, an index correlated with chlorophyll content [18], for determining the progression of the hybrid weakness was also evaluated. The occurrence of cell death and H₂O₂ accumulation was also evaluated, and the expression of disease resistance and photosynthesis-related genes in the leaves of F₁ hybrids exhibiting hybrid weakness were analyzed.

2. Results

2.1. Hybrid Weakness Phenotypes

The *Oryza sativa* Indian cultivars 'A.D.T.14' and 'P.T.B.7' carry homozygous *Hwa1-1* and *Hwa2-1* alleles, respectively. All the F₁ hybrids of a cross between 'A.D.T.14' and 'P.T.B.7' exhibited dwarfism, reduced tiller number, and leaf yellowing (Figure 1). Increases in the height of the F₁ hybrids nearly halted at 50 days after sowing (DAS), whereas that of the parents continued increasing (Figure 2A). The progression of plant age in leaf number in the F₁ hybrids was the same as that in both parents (Figure 2B). The tiller number of both parents continued increasing and reached >35 tillers at 70 DAS, whereas that of the F₁ hybrids increased little and only reached five tillers by 70 DAS (Figure 2C). In addition, both parents headed by 80 DAS, whereas none of the F₁ hybrids had started heading after 140 DAS (Figure 1).

Leaf yellowing was first observed in the F₁ hybrids that had developed seventh or eighth leaves at 30 DAS. Afterward, the leaves turned yellow sequentially, from the lower to the upper leaves. At 60 DAS, the fourth, fifth, and sixth leaves of the F₁ hybrids turned yellow, starting from the leaf tip, and progressing toward the leaf base, whereas those of both parents remained green (Figure 3A–C). Meanwhile, the SPAD values of the fourth, fifth, and sixth leaves of the F₁ hybrids were lower than those of the parents (Figure 3D–F). Furthermore, in the leaves of the F₁ hybrids, the SPAD values of the lower leaves were lower than those of the upper leaves (fourth vs. fifth and sixth leaves and fifth vs. sixth leaves), and within each leaf, the SPAD values of the leaf tips were lower than those of the leaf bases (Figure 3D–F).

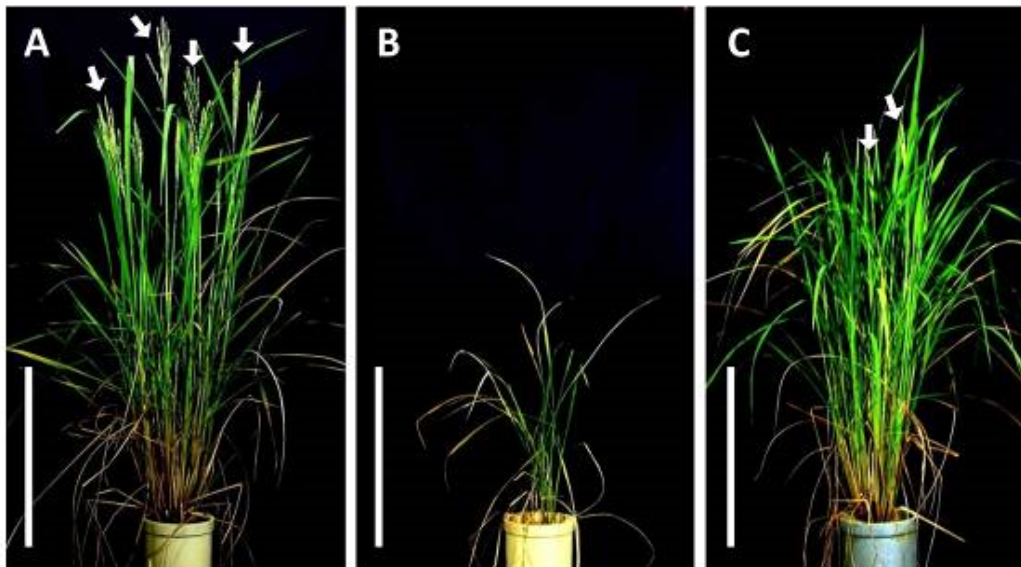


Figure 1. Parental and F₁ hybrid phenotypes at 80 days after sowing. (A) *Oryza sativa* 'A.D.T.14'; (B) F₁ hybrid; and (C) *O. sativa* 'P.T.B.7'. Arrows indicate emerging panicles. Scale bars indicate 50 cm.

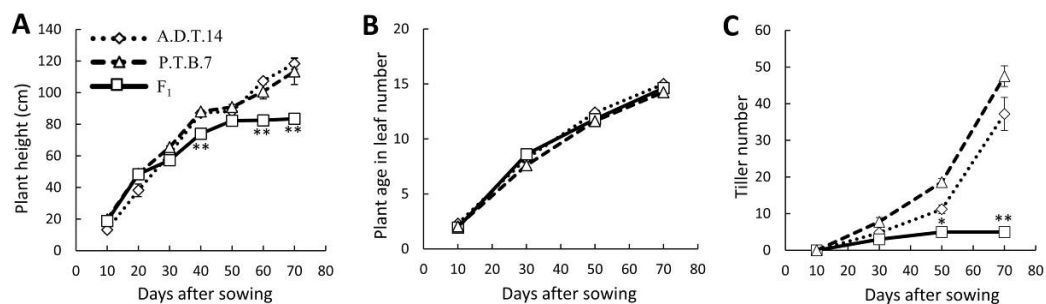


Figure 2. Phenotypic traits of parental and F₁ hybrid rice. (A) plant height; (B) plant age in leaf number; and (C) tiller number. Values and error bars indicate mean \pm SE values ($n = 5$), although some error bars are hidden by the symbols. Mid-parental and hybrids values were compared using two-tailed Student's t-test. Significance: ** $P < 0.01$, * $P < 0.05$.

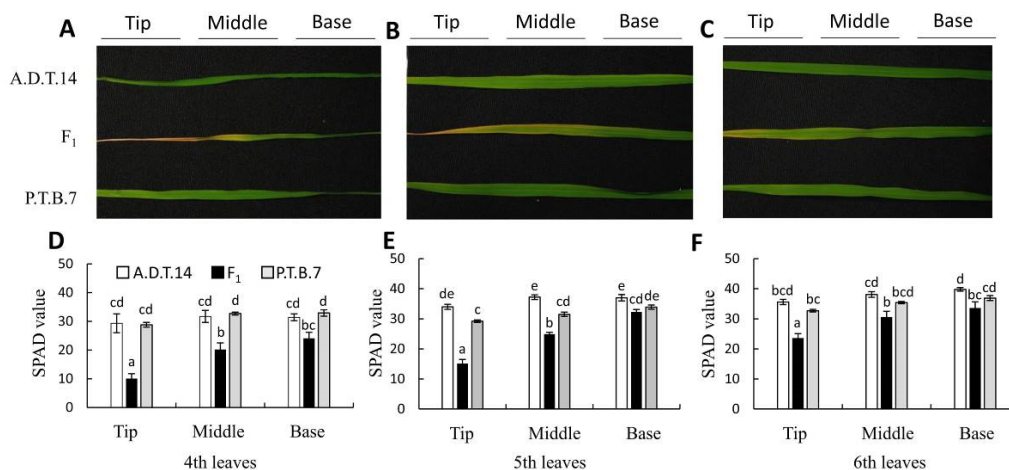


Figure 3. Phenotypes and SPAD values of leaves (fourth to sixth) from parental and F₁ hybrid rice. The phenotypes (A–C) and SPAD values (D–F) of fourth (A, D), fifth (B, E), and sixth (C, F) leaves were assessed at 60 days after sowing. SPAD value was measured at the tip, middle, and base of each leaf. Values and error bars indicate mean \pm SE values ($n = 3$). Different lowercase letters in each plot (D–F) indicate significant differences (Tukey HSD test, $P < 0.05$).

2.2. Cell Death and H₂O₂ Accumulation

The physiological changes that accompanied leaf yellowing were surveyed by analyzing F₁ hybrid leaves that had been classified into four stages based on degree of yellowing (Figure 4A). Chlorophyll content was assessed by SPAD analysis and spectrophotometry. The SPAD values of Stage-1, -2, and -3 leaf tips, Stage-3 leaf middles, and Stage-3 leaf bases were lower than those of Stage-0 leaves (Figure 4B). The SPAD values of Stage-3 leaf tips, Stage-3 leaf middles, and Stage-3 leaf bases were lower than those of Stage-1 leaves (Figure 4B). The SPAD values of Stage-3 leaf middles and Stage-3 leaf bases were lower than those of Stage-2 leaves (Figure 4B). Total chlorophyll content also decreased in all leaf parts (tip, middle, and base) as yellowing progressed (Figure 4C). Because of the usefulness of SPAD value as discussed later, the progression of yellowing of leaves used in the subsequent experiments were evaluated based on SPAD value.

To determine whether cell death occurred in F₁ hybrid leaves, cellular ion leakage, owing to ion permeability by cell death, was measured. Ion leakage increased slightly and significantly in the tips of Stage-2 and Stage-3 leaves, respectively (Figure 4D). Cell death in F₁ hybrid leaves was also evaluated using trypan blue staining, which is used to identify the highly permeable membranes of dead cells. Only Stage-3 leaves contained dead cells (Figure 5A), and the analysis of transverse sections of Stage 3 revealed that the dead cells were located around vascular and epidermal cells (Figure 5B).

Meanwhile, 3,3-diaminobenzidine (DAB) staining revealed the presence of H₂O₂, which, as a reactive oxygen species, is an important regulator of cell death. Plant tissue is stained brown when DAB is oxidized by H₂O₂ into an insoluble polymer. Hydrogen peroxide (H₂O₂) was detected in the leaves of all stages, except Stage 0 (Figure 6).

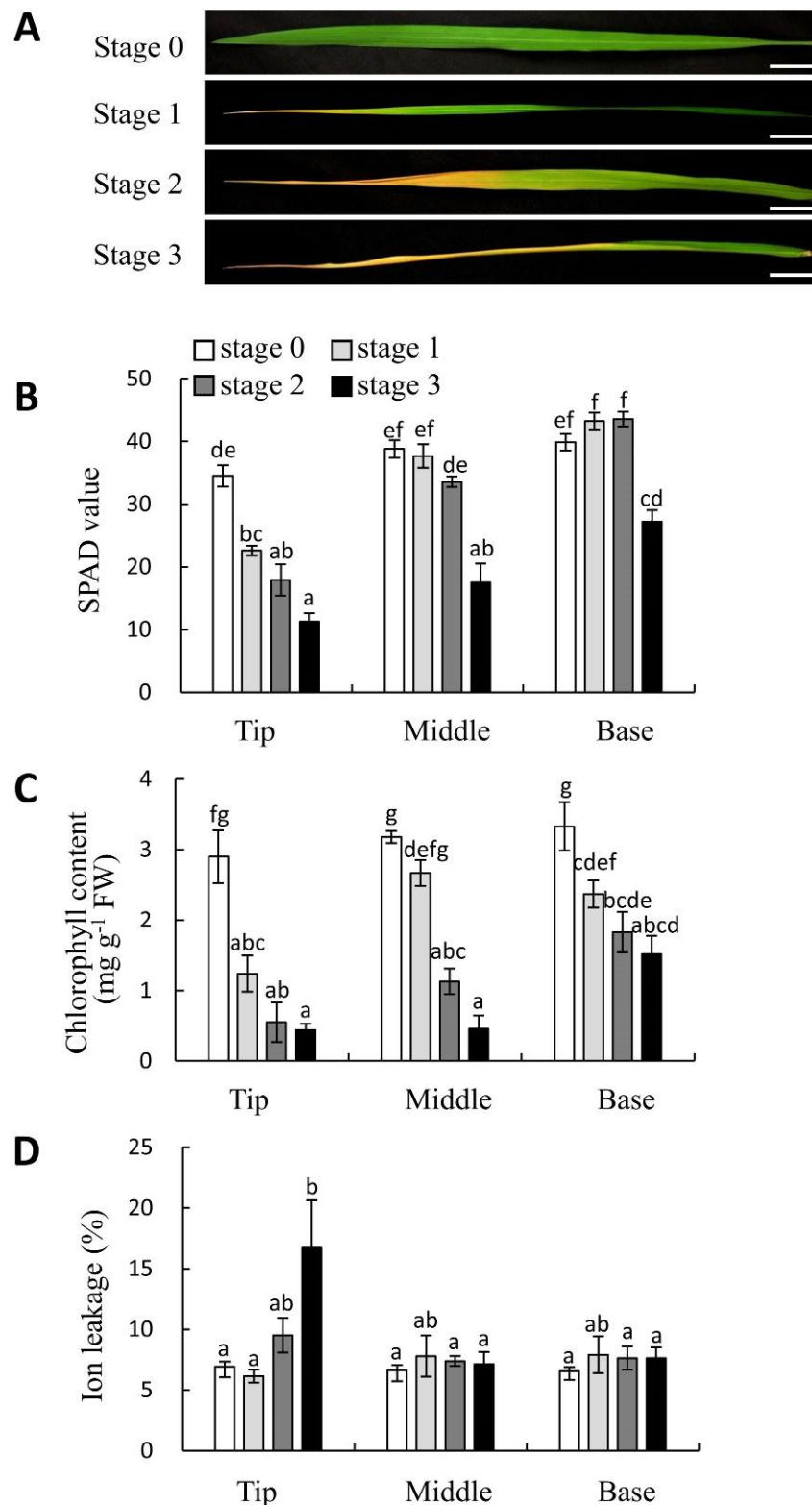


Figure 4. Physiological changes of yellowing hybrid leaves. (A) Stages of yellowing: Stage 0, no yellowing; Stage 1, 1/4 of leaf yellow; Stage 2, 1/2 of leaf yellow; Stage 3, 3/4 of leaf yellow. Scale bars indicate 2 cm. (B) Changes in the SPAD values at the tip, middle, and base of leaves during the progression of yellowing. (C) Changes in chlorophyll content during the progression of yellowing. (D) Changes in ion leakage during the progression of yellowing. Values and error bars (B–D) indicate mean \pm SE values ($n = 3$), and different lowercase letters in each plot (B–D) indicate significant differences (Tukey HSD test, $P < 0.05$).

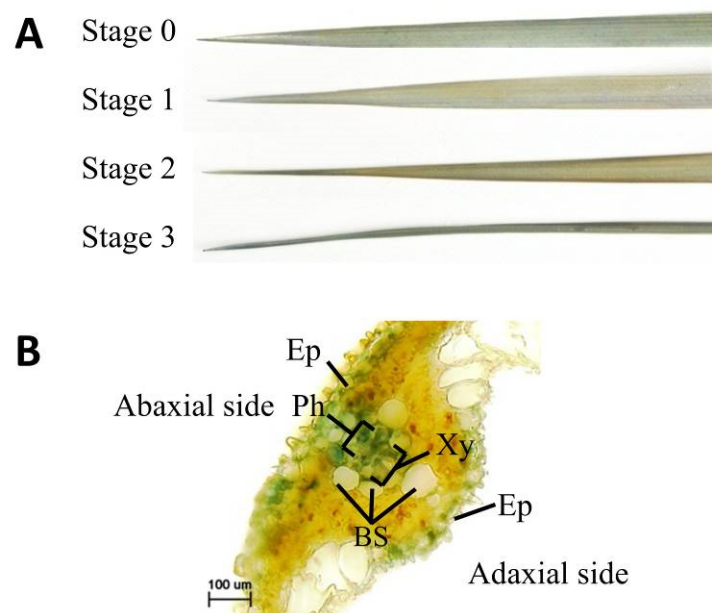


Figure 5. Trypan blue staining of dead cells in F_1 leaves. (A) Stained leaves from each yellowing stage. (B) Transverse section of a stained Stage-3 leaf. Scale bar indicates 100 μm . Xy: Xylem; Ph: Phloem; Ep: Epidermal cell; BS: Bundle sheath cell.



Figure 6. Presence of reactive oxygen species in hybrid leaves. 3,3-diaminobenzidine (DAB) staining was used to detect H_2O_2 . Scale bars indicate 1 cm.

2.3. Hybrid Weakness-Related Gene Expression

At 70 DAS, the 11th (Stage 3) and 13th (Stage 0) leaves of the parents and F_1 offspring were collected for gene expression analysis (Figure 7). The 13th leaves of both the parents and hybrids were entirely green, as indicated by high SPAD values, even though the SPAD values of the F_1 hybrids were somewhat lower than those of either parent (Figure 7A,C). Meanwhile, the 11th leaves of the F_1 hybrids exhibited significant yellowing, as indicated by low SPAD values, whereas those of both parents were entirely green, as indicated by high SPAD values (Figure 7B,D).

The expression of 11 disease resistance-related genes and four photosynthesis-related genes were surveyed (Table 1 and Table S1). The PR1 genes (PR1A and PR1B), the expression of which is induced by salicylic acid [19,20], were upregulated in the 11th leaves of the F_1 hybrids (Figure 8), as were

several PR2 genes (Gns5, Gns2, and OsEGL2), which encode glucanase-related proteins that degrade fungal cell walls [21] (Figure 8). Meanwhile, of several genes that encode chitinase-related proteins (PR4, CHT9, CHT11, and RIXI), which also degrade fungal cell walls [22], PR4, CHT9, and RIXI were all upregulated in the 11th leaves of the F₁ hybrids; however, only PR4 was upregulated significantly (Figure 8). The expression of ACO2, which encodes an enzyme related to ethylene production [23], was similar in the 11th and 13th leaves of the F₁ hybrids (Figure 8). Finally, PDC1, the expression of which is induced by jasmonic acid [24], was upregulated in the 11th leaves of the F₁ hybrids, although not significantly (Figure 8).

Of the four photosynthesis-related genes, PSAF, LHCB, and OsRbcL were somewhat downregulated in the 11th leaves of the F₁ hybrids; however, none of these trends were significant (Figure 8).

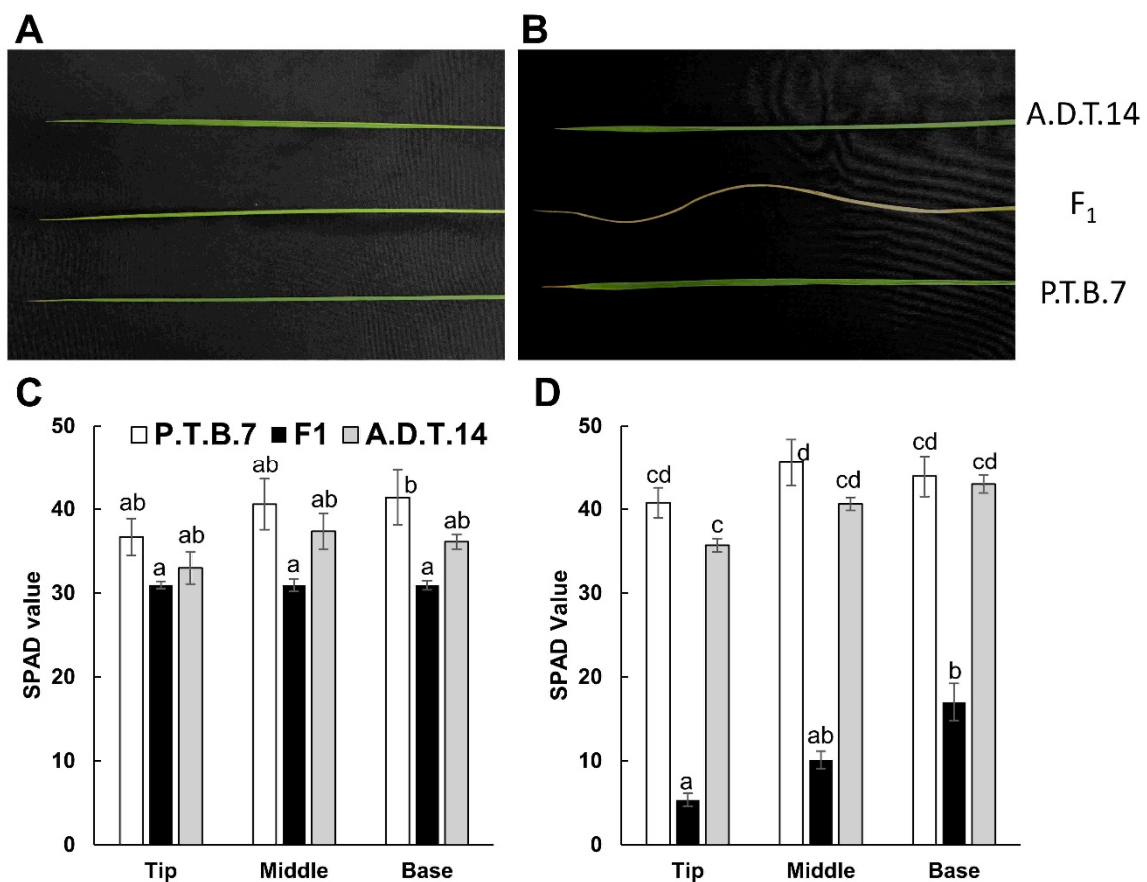


Figure 7. Phenotypes and SPAD values of the parental and F₁ leaves (11th and 13th) used for gene expression analysis. The phenotypes (A, B) and SPAD values (C, D) of 11th (A, C) and 13th (B, D) leaves were assessed at 70 d after sowing. SPAD value was measured at the tip, middle, and base of each leaf. Values and error bars indicate mean \pm SE values ($n = 3$), and different lowercase letters in each plot (C, D) indicate significant differences (Tukey HSD test, $P < 0.05$).

Table 1. Genes analyzed for RT-PCR.

Gene Symbol	RAP-DB locus ID ^a	CGSNL Gene Name ^b	Description
<i>PR1A</i>	Os07g0129200	<i>PATHOGENESIS-RELATED GENE 1A</i>	Similar to Pathogenesis-related protein PR1a
<i>PR1B</i>	Os01g0382000	<i>PATHOGENESIS-RELATED GENE 1B</i>	Similar to Pathogenesis-related protein PRB1-2 precursor
<i>Gns5</i>	Os01g0940700		Similar to Glucan endo-1,3-beta-glucosidase GII precursor
<i>Gns2</i>	Os01g0944900		Similar to Glucan endo-1,3-beta-D-glucosidase
<i>OsEGL2</i>	Os01g0942300		Similar to Beta glucanase precursor
<i>PR4</i>	Os11g0592200	<i>PATHOGENESIS-RELATED GENE 4</i>	Similar to Chitin-binding allergen Bra r 2
<i>CHT9</i>	Os05g0399400	<i>CHITINASE 9</i>	Chitinase 9
<i>CHT11</i>	Os03g0132900	<i>CHITINASE 11</i>	Similar to Chitinase 11
<i>RIXI</i>	Os11g0701800		Chitinase III C10701-rice (Class III chitinase homologue)
<i>ACO2</i>	Os09g0451000	<i>AMINOCYCLOPROPANE-1-CARBOXYLIC ACID OXIDASE 2</i>	Similar to 1-aminocyclopropane-1-carboxylase 1
<i>PDC1</i>	Os05g0469600	<i>PYRUVATE DECARBOXYLASE 1</i>	Similar to Pyruvate decarboxylase
<i>PSAF</i>	Os03g0778100	<i>PHOTOSYSTEM I SUBUNIT</i>	Similar to Photosystem-1 F subunit
<i>LHCB</i>	Os03g0592500		Similar to Photosystem II type II chlorophyll a/b binding protein
<i>OsRbcL</i>	Os06g0598500		Similar to Ribulose bisphosphate carboxylase large chain precursor
<i>Fd1</i>	Os08g0104600		Ferredoxin I, chloroplast precursor
<i>Actin</i>	Os05g0438800		Similar to Actin1

^a Identity of each gene was referenced using the Rice Annotation Project database (<https://rapdb.dna.affrc.go.jp/>); ^b CGSNL (Committee on Gene Symbolization, Nomenclature and Linkage, Rice Genetics Cooperative) gene names were referenced using Oryzabase (<https://shigen.nig.ac.jp/rice/oryzabase/>) [25].

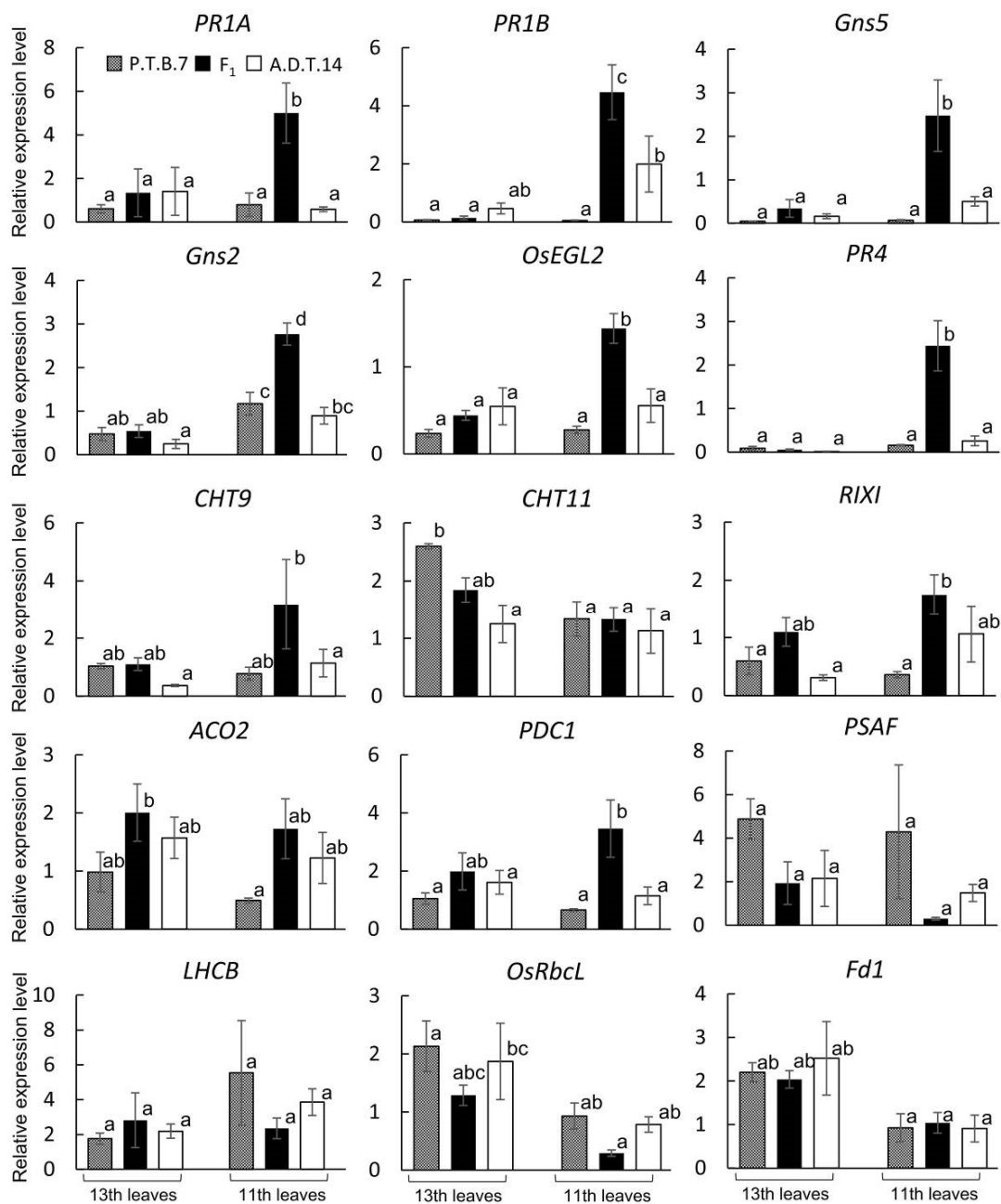


Figure 8. Relative gene expression levels of parental and F₁ hybrid leaves between 'P.T.B.7' and 'A.D.T.14'. Values and error bars indicate mean \pm SE values ($n = 3$), and different lowercase letters in each plot indicate significant differences (Tukey HSD test, $P < 0.05$).

3. Discussion

Oka [4] reported that F₁ hybrids that exhibit hybrid weakness associated with the *HWA1* and *HWA2* loci exhibit growth termination and leaf yellowing after the seedlings developed three or four leaves. However, the plant growth phenotypes were not described in detail. In contrast, the present study determined that F₁ hybrids from the cross of 'A.D.T.14' and 'P.T.B.7' rice exhibited limited growth and tiller number, as well as and leaf yellowing (Figures 1–3). Even though leaf yellowing was also reported by Oka [4], the timing of the yellowing process was different [4]. In the present study, leaf yellowing was observed in F₁ hybrids that had developed seven or eight leaves at 30 DAS and, furthermore, was associated with the downregulation of photosynthesis-related genes (Figure 8).

In *O. sativa*, three other gene sets have been reported to cause hybrid weakness, and the phenotypes associated with each system are different. More specifically, the hybrid weakness associated with the *HWC1* and *HWC2* loci is characterized by short stature, short roots, and rolled leaves [26], whereas that associated with the *HWI1* and *HWI2* loci is characterized by short stature and impaired root formation [2], and that associated with the *HW3* and *HW4* loci is characterized by short culms, fewer panicles, pale green leaves, and chlorotic leaf spots [3]. Remarkably, leaf yellowing has only been reported for the hybrid weakness associated with the *HWA1* and *HWA2* loci. Together, these reports suggest that either the causal genes of each system have different functions or the processes downstream of the causal gene interactions are different.

In the present study, the usefulness of SPAD value for determining the progression of leaf yellowing during hybrid weakness associated with the *HWA1* and *HWA2* loci were evaluated. SPAD values generally corresponded with leaf yellowing (Figure 4A,B) but failed to identify significant differences between the chlorophyll content of Stage-0 leaves and that of either the bases of Stage-1 leaves or the middles or bases of Stage-2 leaves. These results indicate that spectrophotometry is more sensitive than SPAD values to changes in chlorophyll content (Figure 4B,C). However, it is important to note that, because SPAD value accurately reflected degree of leaf yellowing and because spectrophotometry requires leaf destruction (Figure 4), SPAD value measurement is an effective and nondestructive method that can be used to quickly and easily evaluate hybrid weakness associated with the *HWA1* and *HWA2* loci.

The hybrid weakness phenotype that was studied by the present study also exhibited cell death in the yellow leaves (Figures 4D and 5). Similarly, the hybrid weakness associated with the *HWI1* and *HWI2* loci involved cell death at the basal nodes [2], and the hybrid weakness associated with the *HW3* and *HW4* loci involved cell death in leaves [3]. Cell death has been also detected in the leaves of intraspecific *Arabidopsis* hybrids that exhibit hybrid necrosis [7,27] and in the leaves, stems, and roots of interspecific *Nicotiana* hybrids that exhibit hybrid lethality [28,29]. Therefore, despite differences in localization, cell death appears to be a common feature of hybrid weakness in plants.

In the present study, cell death was only detected in Stage-2 and Stage-3 leaves, which indicates that the timing of cell death does not coincide with that of either leaf yellowing or reductions in SPAD value or chlorophyll content (Figure 4). On the other hand, H_2O_2 was detected in Stage-1, -2, and -3 leaves that exhibited yellow leaf tips and low SPAD values (Figure 6). H_2O_2 commonly triggers plant cell death during hypersensitive reactions, senescence, abiotic stress responses, and development [30–32]. We detected that reactive oxygen species would lead to cell death on hybrid weakness by *HWA1* and *HWA2*.

In many cases of hybrid weakness, one of the causal genes encodes an *R* gene, and the interaction of the *R* gene with another causal gene triggers an autoimmune response [7,27,33,34]. In the hybrid weakness associated with the *HWI1* and *HWI2* loci, the causal genes include the LRR-RLK gene (*R* gene) and a subtilisin-like protease gene, respectively, and the interaction of the causal genes results in an autoimmune response [2]. Meanwhile, in the hybrid weakness associated with the *HW3* and *HW4* loci, *HW3* encodes a calmodulin-binding protein, and even though the gene is a defense-response gene, not an *R* gene, the interaction of *HW3* with *HW4* results in an autoimmune response [3]. Furthermore, in the hybrid weakness associated with the *HWA1* and *HWA2* loci, a candidate region, which harbored both loci, also contained 12 *R* genes, along with many other genes [17]. During hypersensitivity reactions, reactive oxygen species are produced, thereby mediating cell death, chloroplast disruption, and the upregulation of defense-related genes [35,36]. In the present study, cell death was detected in the F_1 leaves after H_2O_2 generation and leaf yellowing (Figure 3, Figure 5, and Figure 6), the yellow leaves of the F_1 hybrids exhibited upregulated defense-related genes (Figure 8). These results suggest that the hybrid weakness associated with the *HWA1* and *HWA2* loci involves hypersensitive reaction-like responses. However, because leaf senescence is also associated with H_2O_2 production, cell death, the upregulation of certain defense genes, and leaf yellowing [37], it is possible that the hybrid weakness associated with the *HWA1* and *HWA2* loci involves premature senescence. Additional molecular

studies will reveal the exact mechanism underlying the hybrid weakness associated with the *HWA1* and *HWA2* loci.

4. Materials and Methods

4.1. Plant Materials and Growth Conditions

The *Oryza sativa* Indian cultivars ‘A.D.T.14’ (*indica* [17]), which is homozygous for the *Hwa1-1* allele, and ‘P.T.B.7’ (*aus* [17]), which is homozygous for the *Hwa2-1* allele, were crossed to generate F₁ hybrid offspring. The genotypes of the two cultivars were previously reported by Oka [4]. F₁ seeds were obtained by crossing ‘P.T.B.7’ (♀) and ‘A.D.T.14’ (♂) parents. Seeds of ‘A.D.T.14’, ‘P.T.B.7’, and the F₁ offspring were sown on 17 July 2011. After the seeds were germinated on moistened filter paper in Petri dishes, the seedlings were transplanted to soil (Sukoyaka-Jinko-Baido; Yanmar Co., Ltd., Osaka, Japan) in Wagner pots of 1/5000 a. The seedlings were grown under natural light conditions in a greenhouse at Osaka Prefecture University, Sakai, Japan. The temperature and humidity of the greenhouse were recorded using a data logger (Ondotori; T&D Co., Ltd., Matsumoto, Japan), and the plants were fertilized weekly using Otsuka-A prescription (OAT Agrio Co., Ltd., Tokyo, Japan), which contained 18.6 mM N, 5.1 mM P, 8.6 mM K, 8.2 mM Ca, and 0.4 mM Mg. The plants were cultivated for 140 DAS to survey plant height, plant age in leaf number, tiller number, days to heading, and SPAD value. The plant height was measured from the surface of the soil to the tip of the tallest leaves. To evaluate the relationship between leaf yellowing and physiology, the leaves were classified according to degree of leaf yellowing. Leaves in which 0%, 25%, 50%, or > 75% of the blade had turned yellow were assigned to Stages 0, 1, 2, and 3, respectively (Figure 4A). These leaves classified according to degree of leaf yellowing were used to measure SPAD value and chlorophyll content, as well as to detect dead cells and H₂O₂. Parts of seedlings were cultivated in Wagner pots of 1/10,000 a in an incubator (14 h natural light and 10 h dark, 28 °C, light intensity: 512 μmol m⁻² s⁻¹), and at 70 DAS, these plants were used as material for gene expression analysis.

4.2. SPAD and Chlorophyll Measurement

A SPAD meter (SPAD-502; Konica Minolta, Inc., Tokyo, Japan) was used to measure the SPAD values of the leaves without causing damage. SPAD values were obtained from the tip, middle, and base of each leaf. Meanwhile, total chlorophyll content was measured using a previously described spectrophotometric method [38]. Briefly, the leaves were cut into small pieces, weighed, treated with 20 mL 80% acetone, and ground using a pestle until bleached. The resulting solutions were transferred to 1.5 mL tubes and centrifuged at 10,000 g for 5 min. Each supernatant was transferred to a cuvette, and the absorbance of each supernatant was measured at 663.6 and 646.6 nm, after the spectrophotometer (V-530; JASCO Corp., Hachioji, Japan) was zeroed at 750 nm. Total chlorophyll concentration (mg g⁻¹ FW) was calculated using the following equation: [(17.76 × OD_{646.6} + 7.34 × OD_{663.6}) × extraction volume in a cuvette]/fresh weight (g).

4.3. Ion leakage Measurement

Ion leakage was measured, as described previously [39]. Leaf disks (3 cm²) were taken from the tips, middles, and bases of the leaves, floated for 5 min in water that contained 0.2% (v/v) Tween 20 for removing ion generating on making leaf disks, transferred to Petri dishes that contained fresh water with Tween 20 (0.2%), and incubated for 3 h for leaking out ions by cell death. Their conductivity (value A) of the solutions was measured using a conductivity meter (Twin Cond B-173; Horiba, Ltd., Kyoto, Japan). The leaf disks were then incubated at 95 °C for 25 min, for leaking out ions of whole leaf disks by destroying whole organization, and cooled to room temperature, and their conductivity of the solutions was also measured (value B). Finally, ion leakage (%) was calculated using the following equation: (value A/value B) × 100%.

4.4. Trypan Blue Staining

Trypan blue staining was performed as described previously [40]. Detached leaves were stained by boiling for 8 min in a 1:1 (v:v) mixture of ethanol and lactophenol (i.e., alcoholic lactophenol) that contained 0.1 mg ml⁻¹ trypan blue, cleared in 70% chloral hydrate solution overnight, and then preserved in 70% glycerol. Trypan blue stains dead cells. Transverse slices were prepared using a hand-section method and visualized using a light microscope (Olympus BX50; Olympus, Co. Ltd., Tokyo, Japan).

4.5. Detection of Hydrogen Peroxide Accumulation

Hydrogen peroxide was detected visually, using previously described methods [41]. Briefly, leaves were soaked in a 3,3-diaminobenzidine (DAB) solution for 24 h, transferred to boiling 96% ethanol until bleaching, and then visualized. The presence of H₂O₂ was indicated by brown staining.

4.6. Real-Time qRT-PCR

Total RNA was isolated from leaves using an RNAiso PLUS kit (Takara Bio, Inc., Shiga, Japan), according to the manufacturer's protocol and then treated with RNase-free DNase (Promega Co., Madison, USA), and first-strand cDNA was synthesized from total RNA (2 µg) using oligo (dT)₁₈ primers and ReverTra Ace (Toyobo Co., Ltd., Osaka, Japan). Real-time RT-PCR was carried out to analyze the expression of 11 defense-related genes and four photosynthesis-related genes (Table 1), using *Actin* as an internal control. The primers used to amplify *PR1A*, *PR1B*, *Gns5*, *PR4*, and *Actin* had been reported previously [42], and the other primers were designed based on RAP-DB locus ID using the Primer-BLAST design tool [43] (Table S1). Real-time RT-PCR was performed in 20 µL reaction mixtures that contained 10 µL KAPA SYBR FAST qPCR Master Mix (2×) ABI PRISM (Takara Bio), 10 µM of each forward and reverse primer (0.4 µL each), and 1 µL cDNA template, and the real-time PCR amplification was performed under the following conditions: Initial denaturation at 94 °C for 10 min, followed by 40 cycles of 15 s at 94 °C and 1 min at 60 °C, with a final 30 s extension at 72 °C using an Applied Biosystems 7300 Real-Time PCR System (Applied Biosystems, Foster, CA, USA). The results were analyzed using ABI Prism software (Applied Biosystems). Each gene expression level was divided by the expression level of *Actin* to calculate relative expression level.

4.7. Statistical Analysis

Data were analyzed using SPSS (version 22; IBM, Co., Armonk, USA). Tukey HSD tests were used to compare SPAD, chlorophyll content, and ion leakage values, and two-tailed Student's t-tests were used to compare mid-parental (mean of 'A.D.T.14' and 'P.T.B.7') and hybrid values of plant height, foliar age, and tiller number.

Supplementary Materials: The following are available online at <http://www.mdpi.com/2223-7747/8/11/450/s1>, Table S1: Real-time RT-PCR primers.

Author Contributions: Conceptualization, K.I., T.K., and T.T.; formal analysis, K.S.; funding acquisition, K.I., T.K., and T.T.; investigation, K.S. and T.I.; resources, K.I.; supervision, K.I., T.K., T.M., M.O., and T.T.; writing—original draft, K.S.; writing—review and editing, T.T.

Funding: This research was funded by JSPS KAKENHI (grant no. JP24580009) from the Japan Society for the Promotion of Science.

Acknowledgments: We are grateful to the Genebank of the National Institute of Agrobiological Sciences (Tsukuba, Japan) for providing seeds of the parent lines ('A.D.T.14' and 'P.T.B.7'). We would like to thank Editage (www.editage.com) for English language editing.

Conflicts of Interest: The authors declare no conflict of interest.

References

1. Amemiya, A.; Akemine, H. Biochemical genetic studies on the root growth inhibiting complementary lethal in rice plant (Studies on the embryo culture in rice plant. 3). *Bull. Natl. Inst. Agric. Sci.* **1963**, *10*, 139–226.
2. Chen, C.; Chen, H.; Lin, Y.S.; Shen, J.B.; Shan, J.X.; Qi, P.; Shi, M.; Zhu, M.Z.; Huang, X.H.; Feng, Q.; et al. A two-locus interaction causes interspecific hybrid weakness in rice. *Nat. Commun.* **2014**, *5*, 3357. [[CrossRef](#)] [[PubMed](#)]
3. Fu, C.Y.; Wang, F.; Sun, B.R.; Liu, W.G.; Li, J.H.; Deng, R.F.; Liu, D.L.; Liu, Z.R.; Zhu, M.S.; Liao, Y.L.; et al. Genetic and cytological analysis of a novel type of low temperature-dependent intrasubspecific hybrid weakness in rice. *PLoS ONE* **2013**, *8*, e73886. [[CrossRef](#)] [[PubMed](#)]
4. Oka, H.I. Phylogenetic differentiation of cultivated rice. XV Complementary lethal genes in rice. *Jpn. J. Genet.* **1957**, *32*, 83–87. [[CrossRef](#)]
5. Tezuka, T.; Marubashi, W. Genomic factors lead to programmed cell death during hybrid lethality in interspecific hybrids between *Nicotiana tabacum* and *N. debneyi*. *SABRAO J. Breed Genet.* **2006**, *38*, 69–81.
6. Inai, S.; Ishikawa, K.; Nunomura, O.; Ikehashi, H. Genetic analysis of stunted growth by nuclear-cytoplasmic interaction in interspecific hybrids of *Capsicum* by using RAPD markers. *Theor. Appl. Genet.* **1993**, *87*, 416–422. [[CrossRef](#)]
7. Bomblies, K.; Lempe, J.; Epple, P.; Warthmann, N.; Lanz, C.; Dangl, J.L.; Weigel, D. Autoimmune response as a mechanism for a Dobzhansky-Muller-type incompatibility syndrome in plants. *PLoS Biol.* **2007**, *5*, e236. [[CrossRef](#)]
8. Tsunewaki, K. Monosomic and conventional analyses in common wheat. III Lethality. *Jpn. J. Genet.* **1960**, *35*, 71–75. [[CrossRef](#)]
9. Tsunewaki, K. Aneuploid analysis of hybrid necrosis and hybrid chlorosis in tetraploid wheats using the D genome chromosome substitution lines of durum wheat. *Genome* **1992**, *35*, 594–601. [[CrossRef](#)]
10. Silow, R.A. The comparative genetics of *Gossypium anomalum* and the cultivated Asiatic cottons. *J. Genet.* **1941**, 259–358. [[CrossRef](#)]
11. Reiber, J.M.; Neuman, D.S. Hybrid weakness in *Phaseolus vulgaris* L. II. Disruption of root-shoot integration. *J. Plant Growth Regul.* **1999**, *18*, 107–112. [[CrossRef](#)] [[PubMed](#)]
12. Bateson, W. Heredity and variation in modern science. In *Darwin and Modern Science*; Seward, A.C., Ed.; Cambridge University Press: Cambridge, UK, 1909; pp. 85–101.
13. Dobzhansky, T. *Genetics and the Origin of Species*; Columbia University Press: New York, NY, USA, 1937.
14. Muller, H.J. Isolating mechanisms, evolution, and temperature. *Biol. Symp.* **1942**, *6*, 71–124.
15. Mizuno, N.; Hosogi, N.; Park, P.; Takumi, S. Hypersensitive response-like reaction is associated with hybrid necrosis in interspecific crosses between tetraploid wheat and *Aegilops tauschii* Coss. *PLoS ONE* **2010**, *5*, e11326. [[CrossRef](#)] [[PubMed](#)]
16. Okada, M.; Yoshida, K.; Takumi, S. Hybrid incompatibilities in interspecific crosses between tetraploid wheat and its wild diploid relative *Aegilops umbellulata*. *Plant Mol. Biol.* **2017**, *95*, 625–645. [[CrossRef](#)]
17. Ichitani, K.; Taura, S.; Tezuka, T.; Okiyama, Y.; Kuboyama, T. Chromosomal location of *HWA1* and *HWA2*, complementary hybrid weakness genes in rice. *Rice* **2011**, *4*, 29–38. [[CrossRef](#)]
18. Markwell, J.; Osterman, J.C.; Mitchell, J.L. Calibration of the Minolta SPAD-502 leaf chlorophyll meter. *Photosyn. Res.* **1995**, *46*, 467–472. [[CrossRef](#)]
19. Agrawal, G.K.; Rakwal, R.; Jwa, N.S.; Agrawal, V.P. Signalling molecules and blast pathogen attack activates rice *OsPR1a* and *OsPR1b* genes: A model illustrating components participating during defence/stress response. *Plant Physiol. Biochem.* **2001**, *39*, 1095–1103. [[CrossRef](#)]
20. Van Loon, L.C.; Rep, M.; Pieterse, C.M.J. Significance of inducible defense-related proteins in infected plants. *Annu. Rev. Phytopathol.* **2006**, *44*, 135–162. [[CrossRef](#)]
21. Romero, G.O.; Simmons, C.; Yaneshita, M.; Doan, M.; Thomas, B.R.; Rodriguez, R.L. Characterization of rice endo- β -glucanase genes (Gns2–Gns14) defines a new subgroup within the gene family. *Gene* **1998**, *223*, 311–320. [[CrossRef](#)]
22. Klarzynski, O.; Plesse, B.; Joubert, J.-M.; Yvin, J.-C.; Kopp, M.; Kloareg, B.; Fritig, B. Linear β -1,3 glucans are elicitors of defense responses in tobacco. *Plant Physiol.* **2000**, *124*, 1027–1038. [[CrossRef](#)]
23. Kende, H. Ethylene biosynthesis. *Annu. Rev. Plant. Biol.* **1993**, *44*, 283–307. [[CrossRef](#)]

24. Sugimori, M.; Kiribuchi, K.; Akimoto, C.; Yamaguchi, T.; Minami, E.; Shibuya, N.; Sobajima, H.; Cho, E.M.; Kobashi, N.; Nojiri, H.; et al. Cloning and characterization of cDNAs for the jasmonic acid-responsive genes *RRJ1* and *RRJ2* in suspension-cultured rice cells. *Biosci. Biotechnol. Biochem.* **2002**, *66*, 1140–1142. [[CrossRef](#)]
25. McCouch, S.R. Gene nomenclature system for rice. *Rice* **2008**, *1*, 72–84. [[CrossRef](#)]
26. Saito, T.; Ichitani, K.; Suzuki, T.; Marubashi, W.; Kuboyama, T. Developmental observation and high temperature rescue from hybrid weakness in a cross between Japanese rice cultivars and Peruvian rice cultivar 'Jamaica'. *Breed. Sci.* **2007**, *57*, 281–288. [[CrossRef](#)]
27. Alcázar, R.; García, A.V.; Kronholm, I.; de Meaux, J.; Koornneef, M.; Parker, J.E.; Reymond, M. Natural variation at Strubbelig Receptor Kinase 3 drives immune-triggered incompatibilities between *Arabidopsis thaliana* accessions. *Nat. Genet.* **2010**, *42*, 1135–1139. [[CrossRef](#)]
28. Tezuka, T.; Marubashi, W. Apoptotic cell death observed during the expression of hybrid lethality in interspecific hybrids between *Nicotiana tabacum* and *N. suaveolens*. *Breed. Sci.* **2004**, *54*, 59–66. [[CrossRef](#)]
29. Yamada, T.; Marubashi, W.; Niwa, M. Apoptotic cell death induces temperature-sensitive lethality in hybrid seedlings and calli derived from the cross of *Nicotiana suaveolens* × *N. tabacum*. *Planta* **2000**, *211*, 614–622. [[CrossRef](#)]
30. Huysmans, M.; Lema, A.S.; Coll, N.S.; Nowack, M.K. Dying two deaths—Programmed cell death regulation in development and disease. *Curr. Opin. Plant Biol.* **2017**, *35*, 37–44. [[CrossRef](#)]
31. Petrov, V.; Hille, J.; Mueller-Roeber, B.; Gechev, T.S. ROS-mediated abiotic stress-induced programmed cell death in plants. *Front Plant Sci.* **2015**, *6*, 69. [[CrossRef](#)]
32. Woo, H.R.; Kim, H.J.; Nam, H.G.; Lim, P.O. Plant leaf senescence and death—Regulation by multiple layers of control and implications for aging in general. *J. Cell Sci.* **2013**, *126*, 4823. [[CrossRef](#)]
33. Huang, X.; Li, J.; Bao, F.; Zhang, X.; Yang, S. A gain-of-function mutation in the *Arabidopsis* disease resistance gene *RPP4* confers sensitivity to low temperature. *Plant Physiol.* **2010**, *154*, 796–809. [[CrossRef](#)] [[PubMed](#)]
34. Yang, S.; Hua, J. A haplotype-specific resistance gene regulated by *BONZAI1* mediates temperature-dependent growth control in *Arabidopsis*. *Plant Cell* **2004**, *16*, 1060–1071. [[CrossRef](#)] [[PubMed](#)]
35. Coll, N.S.; Epple, P.; Dangl, J.L. Programmed cell death in the plant immune system. *Cell Death Differ.* **2011**, *18*, 1247. [[CrossRef](#)] [[PubMed](#)]
36. Overmyer, K.; Brosché, M.; Kangasjärvi, J. Reactive oxygen species and hormonal control of cell death. *Trends Plant Sci.* **2003**, *8*, 335–342. [[CrossRef](#)]
37. Jajic, I.; Sarna, T.; Strzalka, K. Senescence, stress, and reactive oxygen species. *Plants* **2015**, *4*, 393–411. [[CrossRef](#)]
38. Porra, R.J.; Thompson, W.A.; Kriedemann, P.E. Determination of accurate extinction coefficients and simultaneous equations for assaying chlorophylls a and b extracted with four different solvents: Verification of the concentration of chlorophyll standards by atomic absorption spectroscopy. *Biochim. Biophys. Acta* **1989**, *975*, 384–394. [[CrossRef](#)]
39. Rizhsky, L.; Shulaev, V.; Mittler, R. Measuring programmed cell death in plants. In *Apoptosis Methods and Protocols*; Brady, H.J.M., Ed.; Humana Press: Totowa, NJ, USA, 2004; pp. 179–189.
40. Zhang, H.K.; Zhang, X.; Mao, B.Z.; Li, Q.; He, Z.H. Alpha-picolinic acid, a fungal toxin and mammal apoptosis-inducing agent, elicits hypersensitive-like response and enhances disease resistance in rice. *Cell Res.* **2004**, *14*, 27–33. [[CrossRef](#)]
41. Chandru, H.K.; Kim, E.; Kuk, Y.; Cho, K.; Han, O. Kinetics of wound-induced activation of antioxidative enzymes in *Oryza sativa*: Differential activation at different growth stages. *Plant Sci.* **2003**, *164*, 935–941. [[CrossRef](#)]
42. Yamamoto, E.; Takashi, T.; Morinaka, Y.; Lin, S.; Wu, J.; Matsumoto, T.; Kitano, H.; Matsuoka, M.; Ashikari, M. Gain of deleterious function causes an autoimmune response and Bateson–Dobzhansky–Muller incompatibility in rice. *Mol. Genet. Genomics* **2010**, *283*, 305–315. [[CrossRef](#)]
43. Ye, J.; Coulouris, G.; Zaretskaya, I.; Cutcutache, I.; Rozen, S.; Madden, T.L. Primer-BLAST: A tool to design target-specific primers for polymerase chain reaction. *BMC Bioinform.* **2012**, *13*, 134. [[CrossRef](#)]

